CHARACTERISTICS OF THE SPT100-ML COMPARISONS BETWEEN EXPERIMENTS AND MODELS

L. Garrigues*, C. Pérot†, N. Gascon†, S. Béchu†, P. Lasgorceix†, M. Dudeck†, and J.P. Boeuf*

* *Centre de Physique des Plasmas et Applications de Toulouse*
Université Paul Sabatier
118 route de Narbonne, 31062 Toulouse Cedex 4, FRANCE
† *Laboratoire d'Aérothermique*
2 rue du crital, 45100 Orléans, FRANCE

Abstract

Different modes of oscillations of the current have been experimentally observed on the SPT100-ML, a Stationary Plasma Thruster studied at the French facility PIVOINE. We have used a 1D transient quasineutral hybrid model of the device to study the current-voltage characteristics of the discharge and the low frequency oscillations of the current. The model predictions are in good qualitative agreement with the experiments. The simulations show that different oscillation regimes can coexist for this device.

Nomenclature

B	Magnetic Field [T]
d	Dimension of the Channel [m]
δ	Dirac Function
Δt	Ion Transport Time Step [s]
e	Electric Charge Constant = 1.602×10^{-19} C
E	Electric Field [Vm^{-1}]
f	Ion Distribution Function
φ_e, φ_i	Electron, and Ion Flux [$m^{-2}s^{-1}$]
I_d, I_b	Discharge, and Coils Current [A]
J_e, J_i, J_d	Electron, Ion, and Discharge Current [A]
k_i	Ionization Rate [m^3s^{-1}]
m_e, M	Electron Mass = 9.1×10^{-31} kg, Neutral Atom Mass Xe=131.3 uma
$\dot{m}$	Propellant Mass Flow Rate at the Anode [kgs^{-1}]
μ_e	Axial Electron Mobility [$m^2V^{-1}s^{-1}$]
n_i, N_a, n_p	Ion, Neutral, and Plasma Density [m^{-3}]
σ_e	Electron Conductivity [$\Omega^{-1}.m^{-1}$]
V_d	Applied Voltage [V]
v_0	Neutral Atom Velocity [m/s]
x, v_x	Axial Position, and Axial Velocity [m] and [m/s]

Introduction

In Hall thrusters xenon ions are accelerated through a channel between two concentric dielectric cylinders. The dimensions of the channel are only a few centimeters and the gas density is on the order of 10^{13} cm^{-3} so the charged particles mean free paths are much longer than the device dimensions. A radial magnetic field is applied to the channel in order to decrease the axial electron mean velocity and to increase the number of collisions between electrons and neutral atoms. The magnetic field is large in the exhaust region of the channel and decreases toward the anode which is located at the other end of the channel. The decrease of the axial electron mobility in the exhaust region leads to an increase of the self-consistent electric field in this region. This electric field accelerates the ions toward the exhaust. In contrast to standard ion thrusters, there is no need for accelerating grids in a SPT since the ion acceleration is provided by the plasma electric field. It is believed that performances of Hall thruster are higher than those of conventional ion thrusters because of the smaller recombination of ion on the walls in SPTs[1].

Stationary Plasma Thrusters of the SPT100 family have specific impulse and thrust in the 1600 s and 80 mN range respectively. They are well adapted for north-south station-keeping of Geostationary Earth Orbit telecom satellites[1,2]. New devices with smaller and larger dimensions than the SPT100 are now studied for applications such as telecom constellations on Low Earth Orbit, or for primary propulsion of interplanetary missions[3].

A better understanding of the physical mechanisms occurring in the SPT is still needed in order to optimize the operating conditions and to guide the design of new devices. Numerical models can help improve our understanding of these devices and guide the optimization. Systematic comparisons between experiments and models are also essential for the development of realistic models. We have recently developed a one-dimensional hybrid model of the SPT[4]. This model can reproduce qualitatively well the properties of the device[5]. Now, the aim is to go one step further and to study the ability of the model to give quantitative predictions of the thruster characteristics. A companion paper in these proceedings is dedicated to the study of SPT100 performances[6]. The goal of

this paper is to compare the current voltage characteristics and the low frequency oscillations predicted by the model and measured on a French laboratory model, the SPT100-ML.

The principles of the numerical model and the calculation procedure are briefly discussed in a first part. We describe in a second part the experimental set-up and the thruster. The comparisons between results of the model and experimental measurements are shown and analyzed in the third part. A discussion on the oscillations modes predicted by the model is given in the last section.

Numerical Model and Calculation Procedure

The 1D hybrid model is the same as that described in Ref. [4]. It assumes quasineutrality of the plasma, the ions are described with a microscopic equation (Vlasov) and electrons are treated as a fluid. The principles of the model are summarized below (a more detailed set of equation can be found in Ref. [4], and also in paper [6] of these proceedings, where the only difference is in the numerical resolution of the ion Vlasov equation).

1) ions are in free fall, are not sensitive to the magnetic field, and are created with a constant velocity equal to the neutral velocity at the anode v_0. The ion transport is described with a 1D (in space and velocity) Vlasov equation.

$$\frac{\partial f}{\partial t} + v_x \frac{\partial f}{\partial x} + \frac{e}{M} E \frac{\partial f}{\partial v_x} = n_i N_a k_i \delta(v_x - v_0) \quad (1)$$

This equation is solved with an upwind scheme and time splitting here and in [8] (and is solved with a particle method in [6])

2) the electron are treated as a fluid with continuity, momentum, and energy equations. The electron density is deduced from quasineutrality. The electron momentum equation is supposed to take the simple form $j_e = \sigma_e E$, where j_e is the electron current density, σ_e is the electron conductivity and E the electric field. A simplified form of the energy equation is also used[4-6]. We consider only steady state electron momentum and energy equations since we are interested only in ion and neutral atom time scales.

3) The electric field is obtained from the electron momentum equation ($j_e = \sigma_e E$) using the assumption of quasi-neutrality ($n_i = n_e$).

$$E = -\frac{\varphi_e}{n \mu_e} \quad (2)$$

where the electron flux φ_e is deduced from the ion current (given by Vlasov equation) and from current continuity. In our model, the electron mobility perpendicular to the magnetic field is classical and includes the effects of electron-neutral collisions as well as electron-wall collisions (in a phenomenological way).

4) the neutral transport is fluid, and described with a simple continuity equation with a loss term, and a constant velocity equal to the injection velocity at the anode :

$$\frac{\partial N_a}{\partial t} + v_0 \frac{\partial N_a}{\partial x} = -n_i N_a k_i \quad (3)$$

5) The ion source term ($n_i N_a k_i$) is the product of the electron density by the neutral density and by the ionization rate. To estimate k_i , we have supposed that the electron distribution function is Maxwellian, the electron temperature being deduced form the simplified electron energy equation. Work is also in progress to improve our description of the electron distribution function using Monte Carlo and kinetic models of the electron transport[7].

All the details of the model and boundaries conditions can be found in Ref. [4]. Comparisons with a much more detailed PIC MCC model[8] have shown that this simple hybrid model can reproduce qualitatively well several interesting features of the SPT such as the low frequency oscillations.

Experimental Description

The measurements were made at the PIVOINE test facility, which has been specially designed and built for simulating space environment and carrying out electric propulsion experiments. The vacuum chamber is a stainless steel cylindrical tank, 4 m long and 2.2 m in diameter. The pumping system (dry and cryogenic) keeps the pressure inside the tank lower than 2×10^{-5} mbar for a flow rate of xenon propellant of 5 mg/s. The vacuum chamber systems and parameters are automatically monitored and controlled. Several kinds of plasma diagnostics have been used in the facility since its startup in 1997, including optical fibers, high-speed cameras and electrostatic probes[9,10].

A thrust scale was also designed and built. Its range is 0-500 mN, with a +/-3 mN precision for a 80 mN thrust. A laboratory Hall thruster called SPT100-ML was used in this study (see Fig. 1). Its design is based on the Russian SPT100 (100 mm channel diameter), but the geometrical configuration (channel length, position of the magnetic poles) can be changed for experimental purposes. Another important feature of the SPT100-ML is that the inner and outer electromagnets have each their own power supply, whereas in a flight model, they are in series with the discharge. The SPT100-ML nominal operating point is 300 V discharge voltage, 5 mg/s xenon flow rate at the anode, and 4.5 A coils current. At 2×10^{-5} mbar pressure, the discharge current is then 4.2 A, and the thrust is 80mN[2].

The DC discharge current was measured with a Hall-effect module. The AC current was measured with a resistor shunt and a Tektronic VXI system, at 200kHz sampling rate.

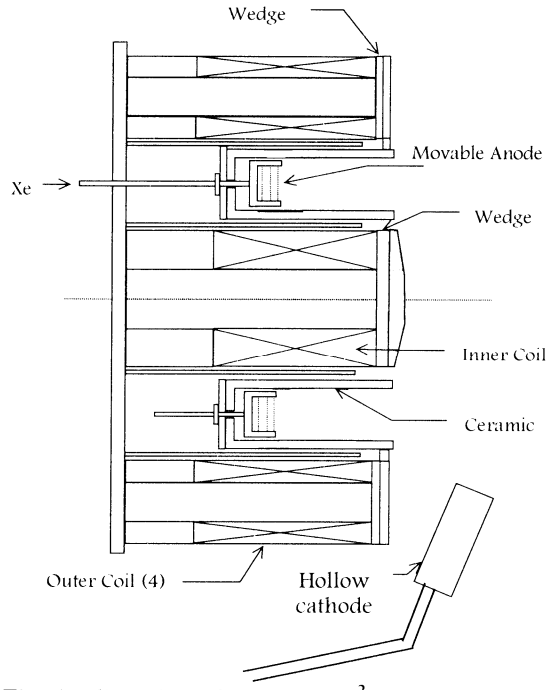

Fig. 1 : Cut of the SPT100-ML[2].

Electrical Characteristics of the SPT100-ML From Measurements and Simulations

We have compared the amplitude and oscillations of the measured and calculated currents in the SPT100-ML for different applied voltages.

The axial profile of the radial magnetic field we use in the simulation in this section (for a coil current of 4.5 A) is shown in Fig. 2.

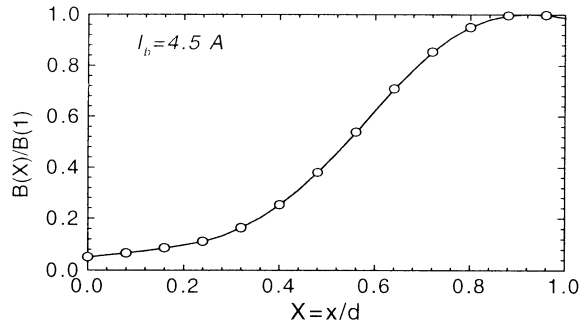

Fig. 2 : Axial distribution of the radial magnetic field used in the simulations.

Since the model in only one-dimensional we cannot take into account the real magnetic field distribution. The curve of Fig. 2 corresponds to a distribution of the measured radial magnetic field averaged over the radius of the channel.

The experiments as well as the model show that the electrical properties of the SPT100-ML exhibits low frequency oscillations in a large range of operating conditions.

Figure 3 displays the variations with applied voltage of the averaged measured current. The minimum and maximum of the current oscillations are also represented in this figure. The anode mass flow rate is 3.8 mg/s.

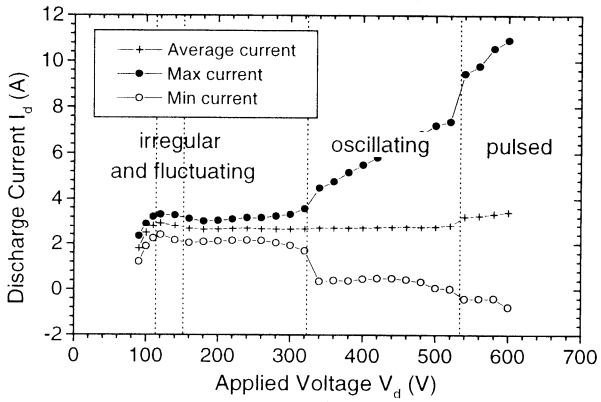

Fig. 3 : Maximum, minimum, and average discharge current obtained experimentally as function of discharge voltage. The xenon mass flow rate is 3.8 mg/s (after Ref. [11]).

The results of Fig. 3 show that one can roughly distinguish three regions in the current voltage characteristic curve (a more detailed analysis is given in Ref. [11]). In the first region corresponding to the [100 V – 300 V] voltage range, the device exhibits small amplitudes irregular fluctuations. Above the "knee" of the I-V characteristic, a main frequency of 20 kHz starts to appear in these fluctuations. In the [300 V – 500 V] voltage range the discharge is in a much more regular oscillating regime, with quasi-sinusoidal low frequency oscillations around 20 kHz. Above 500 V, the current is formed of large amplitude short pulses of very high amplitude, also at a frequency around 20 kHz.

The oscillations in the "oscillating" and "pulsed" regimes of Fig. 3 have been clearly identified in previous work as due to a "breathing" of the front of neutral atoms both in with the help of the simulations[4] and experimentally[12]. The neutral atoms are strongly ionized by electrons when they reach the exhaust plane. This ionization induces a depletion of the neutral atom density, and the neutral atom front moves back inside the channel. During the motion of the front inside the channel, ionization decreases due to the decrease of the electric field and electron energy in the channel. The current then drops and the plasma and discharge current decay. The atoms can then move to the exhaust plane until ionization by energetic electrons starts again. The oscillations are therefore associated with the periodic depletion of the neutral atoms in the exhaust region. The period of the oscillations is related to the time needed by the atoms to cross the high electric region (which is also the region of large radial magnetic field) near the exhaust. Since the length of this region is typically 1 cm (see Fig. 2) and the atom velocity is on the order of 3×10^4

cm/s, the frequency of the oscillations is around 30 kHz.

The current-voltage characteristic curve predicted by the model is represented in Fig. 4 for the same conditions as the experimental results of Fig. 3.

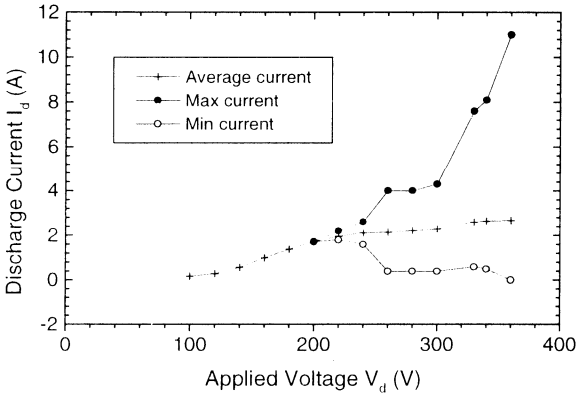

Fig. 4: Maximum, minimum, and average discharge current predicted by the model in the same conditions as Fig. 3.

The results of Fig. 4 show some qualitative agreement with the experimental measurements of Fig. 3. The oscillations start above 200 V, and large amplitude oscillations are observed above 300 V. The average current is in quantitative agreement with the experiment. An important discrepancy between the model and the experimental results concerns the region between 100 V and 200 V where the model predicts a slow increase of the current from 0, around 100 V, to about 2 A, while the measurements give a rather constant average current at about 2 A.

Figure 5 displays typical oscillations regimes predicted by the model along the I-V characteristic of Fig. 4. Between 200 V and 240 V the model predicts small amplitude (regular) oscillations around a frequency of 125 kHz (see Fig. 5a). Between 260 V and 320V, the model predicts hybrid oscillations with a dominant frequency around 25-30 kHz and other components at higher frequencies in the 125 kHz range (Fig. 5b). Above 330 V the oscillations are very regular, quasi-sinusoidal at 18-20 kHz (Fig. 5c). When the voltage increases more, the regime evolves from this "sinusoidal", regular oscillations to a regime similar to the "pulsed" regime of Fig. 3 characterized by short pulses of very large amplitude (Fig. 5d). The model predictions above 330 V therefore seem to correspond very well (at least qualitatively) to the experimental observations of [11] corresponding to the region above 300 V of the experimental I-V characteristic of Fig. 3. We also believe that the model gives a good description of the physical mechanisms responsible for the oscillations in that regime. For lower applied voltages, it is not so clear whether the experimentally observed "irregular and fluctuating" regime of Fig. 3 and the hybrid regime of oscillations predicted by the model really have the same physical meaning.

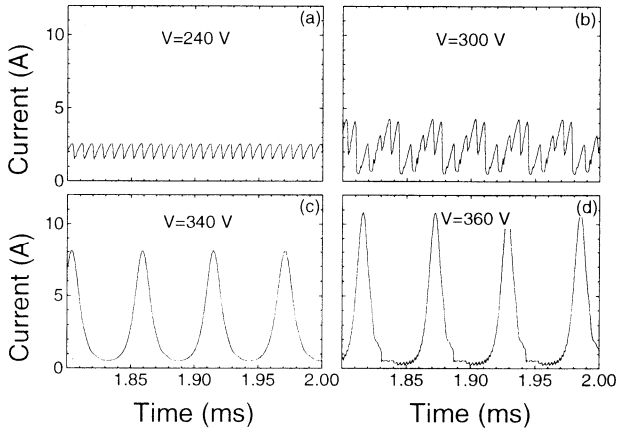

Fig. 5: Time evolution of the calculated current for typical values of the voltage showing the different regimes along the calculated I-V characteristic of Fig. 4.

Coexistence of Different Regimes of Oscillations

The discharge regime predicted by the model can be strongly dependant on the magnetic field profile.

As mentioned above, the 1D model cannot take into account the exact magnetic field distribution, and we have to choose a 1D distribution of the radial magnetic field from the 2D real magnetic field map. In the calculations presented above, we chose to use a value of the radial magnetic field averaged over the radial position between the concentric cylinders. Another possibility is to use a radial magnetic field profile corresponding, e.g., to the measured radial magnetic field along a line parallel to the cylinder axis, and at a radial position located in the middle of the channel. This profile is displayed in Fig. 6, together with the profile used above and also shown in Fig. 2.

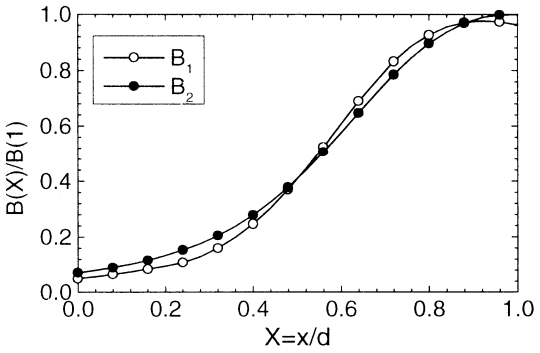

Fig. 6: Two different magnetic profiles used in the calculation. B_1 is the same as in Fig. 2. B_2 corresponds to the axial distribution of the radial magnetic field measured in the middle of the channel.

These two profiles seem very similar. The 1D model was run for this new distribution of the radial mag-

netic field (indicated as B_2, B_1 corresponding to the previous distribution of Fig. 2).

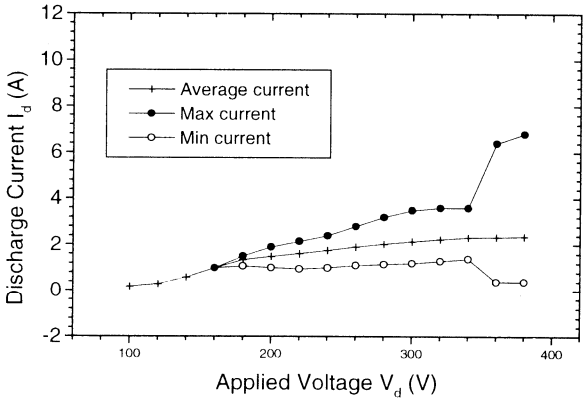

Fig. 7: Maximum, minimum, and average discharge current predicted by the model with the magnetic field profile B_2.

In spite of the similarity between the two profiles, the calculated I-V characteristic curve corresponding to B_2 and displayed in Fig. 7 is different from the I-V curve calculated for the B_1 profile and displayed in Fig. 4. Actually the average currents calculated for both profiles are not significantly different, but the amplitudes and the shapes of the current oscillations are very different in both cases. The typical current waveforms corresponding to the B_2 profile are shown in Fig. 8 and can be compared to those of Fig. 5 for the B_1 profile. We see that for voltages around 200 V (Fig. 8a) we have low amplitude oscillations around 150 kHz, as in Fig. 5. When the voltage increases a lower frequency (~10 kHz) oscillation appears (Fig. 8b). The amplitude of the lower frequency component of the oscillations increases with increasing voltage (Fig. 8c).

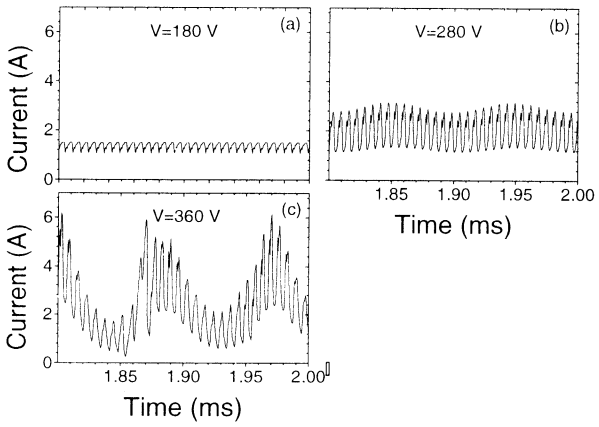

Fig. 8: Time evolution of the calculated current for typical values of the voltage showing the different regimes along the calculated I-V characteristic of Fig. 7.

The space and time variations of the plasma density and neutral atom density in this field configuration show that ionization takes place more deeply in the channel than for the B_1 field configuration. On the other hand, we find as before that the lower frequency oscillations are associated with the transit time of the neutral atoms in the acceleration region. The higher frequency component is associated with instability generated in the anode region, as described in a recent paper[8].

It may seem quite surprising that such a small difference in the magnetic field profile induces a rather large difference in the current oscillation. We find that in some conditions there is not a unique solution to the equations of the model. All the results presented above have obtained assuming a uniform plasma density of 10^9 cm^{-3} in the channel at the beginning of the calculations. We also performed calculations for different initial conditions. For example, we started the calculations with a uniform initial density for the magnetic field profile B_2 and for 340 V and 3.8 mg/s. We reached a steady state similar to the case of Fig. 8c. After steady state was reached we stopped the calculations, and restarted it but using the other field profile B_1, and with the previously calculated plasma density as initial condition. The calculations converged toward a steady state where the current oscillations were different from those of Fig. 5c (and also different from those of Fig. 8c).

It is therefore clear that multiple oscillation regimes may exist for the same conditions and that it is possible in the calculations to go from one regime to the other by imposing a small perturbation in some parameters.

This possibility of bifurcations between different states of the discharge has some qualitative similarities with the experimental observations although it is not possible to relate precisely the results of the model to well defined transitions between different discharge regimes which could be obtained in the experiments.

However a general tendency in the results from the model is that oscillations in the 20 kHz range always occur for large enough voltages, i.e. when the neutral density is strongly depleted in the exhaust region. The higher frequency component, in the 100 kHz range, is not seen when the magnetic field in the anode region is small enough and tend to appear and superimpose to the 20 kHz oscillations when the magnetic field increases in this region. These oscillations are associated with an ionization instability in the anode region and have been described in Ref. [8]. In these conditions of larger magnetic field in the anode region, ionization is important not only in the exhaust region, and the part of ionization occurring deeper in the channel becomes non negligible. These two regimes corresponding to 1) dominant ionization in the exhaust region, and 2) non negligible ionization deeper in the channel may also coexist for the same magnetic field profile. The discharge efficiency and thrust are generally much lower when an important ionization region exists deeper in the channel. For example we

find that the efficiency and thrust of the strong low frequency oscillation regime of Fig. 5c are substantially larger than those corresponding to the hybrid oscillation regime of Fig. 7c (thrust and efficiency of 63 mN and 57% respectively for Fig. 5c, vs 38 mN and 24% for Fig. 7c).

Conclusions

We have studied the low frequency oscillations of a Stationary Plasma Thruster both experimentally and with the help of a one-dimensional hybrid model of the plasma channel. The results from the experiments and models exhibits some striking qualitative similarities which indicate that the model can capture some of the complex physical mechanisms occurring in the device. The model results also show the possibility of coexistence of different discharge regimes for the same conditions. From the model calculations, one can also deduce that the regime of oscillations seems more efficient when the value of the radial magnetic field in the anode region is sufficiently small.
Both model and experiments lead to the conclusion that the low frequency oscillations in the 20 kHz range is due to the periodical depletion of the neutral atom density by ionization in the acceleration zone. The higher frequency oscillations in the 100 kHz range predicted by the model, and their possible relation with instability in the anode region still need to be confirmed by the experiments although recent optical measurements[13] show important emission in the anode region which could be related to an ionization instability.

Acknowledgements

This work was performed in the frame of the Groupement de Recherche CNRS/CNES /SEP/ONERA n° 1184 "Propulsion à Plasma pour Systèmes Orbitaux".

References

[1] J.R. Brophy, J.W. Barnett, J.M. Sankovic, and D.A. Barnhart, "Performance of Stationary Plasma Thruster: SPT-100", *28th AIAA Joint Propulsion Conference*, Nashville, TN, 1992, paper AIAA-92-3155.

[2] S. Béchu, C. Pérot, N. Gascon, P. Lasgorceix, A. Hauser, and M. Dudeck, "Operating Mode Investigation of a Laboratory Stationary Plasma Thruster", *35th AIAA Joint Propulsion Conference*, Los Angeles, CA, 1999, paper AIAA-99-2567.

[3] G. Saccoccia, "European Electric Propulsion Activities", *35th AIAA Joint Propulsion Conference*, Los Angeles, CA, 1999, paper AIAA-99-2158.

[4] J.P. Boeuf, and L. Garrigues, "Low Frequency Oscillations in a Stationary Plasma Thruster", *Journal of Applied Physics* **84**, 3541 (1998).

[5] F. Darnon, L. Garrigues, J.P. Boeuf, A. Bouchoule, and M. Lyszyk, "Spontaneous Oscillations in a Hall Thruster", *IEEE Transactions on Plasma Science* **27**, 98 (1999).

[6] L. Garrigues, I.D. Boyd, and J.P. Boeuf, "Calculations Hall Thruster Performance", *26th International Electric Propulsion Conference*, Kitakyushu, Japan, 1999, paper IEPC-99-098.

[7] V. Latocha, L. Garrigues, P. Degond, and J.P. Boeuf, "Comparisons Between Monte Carlo Simulation and Kinetic Model of Electron Transport in Hall Thruster", *26th International Electric Propulsion Conference*, Kitakyushu, Japan, 1999, paper IEPC-99-111.

[8] L. Garrigues, A. Heron, J.C. Adam, and J.P. Boeuf, "Comparisons Between Hybrid and PIC Models of Stationary Plasma Thruster", *35th AIAA Joint Propulsion Conference*, Los Angeles, CA, 1999, paper AIAA-99-2297.

[9] F. Darnon, A. Bouchoule, M. Lyszyk, S. Béchu, P. Lasgorceix, L. Magne, D. Pagnon, M. Touzeau, and S. Roche, "Time Resolved Characterization of the Plasma and the Plume of a SPT Thruster", *35th AIAA Joint Propulsion Conference*, Los Angeles, CA, 1999, paper AIAA-99-2428.

[10] C. Pérot, , S. Béchu, P. Lasgorceix, M. Dudeck, L. Garrigues, and J.P. Boeuf, " Characterization of a Laboratory Hall Thruster with Electrical Probes and Comparisons with a 2D Hybrid PIC-MCC Model", *35th AIAA Joint Propulsion Conference*, Los Angeles, CA, 1999, paper AIAA-99-2716.

[11] N. Gascon, C. Pérot, G. Bonhomme, X. Caron, S. Béchu, P. Lasgorceix, B. Izrar, M. Dudeck, "Signal Processing and Non Linear Behavior of Stationary Plasma Thruster : First Results", *35th AIAA Joint Propulsion Conference*, Los Angeles, CA, 1999, paper AIAA-99-2427.

[12] F. Darnon, C. Kadlec-Philippe, A. Bouchoule, M. Lyszyk, "Dynamic Plasma and Plume Behavior of SPT Thrusters", *34th AIAA Joint Propulsion Conference*, Cleveland, OH, 1998, paper AIAA-98-3644.

[13] N.B. Meezan, D.P. Schmidt, W.A. Hargus Jr., and M.A. Capelli, "Optical Study of Anomalous Electron Transport in a Laboratory Hall Thruster", *35th AIAA Joint Propulsion Conference*, Los Angeles, CA, 1999, paper AIAA-99-2284.